Optimization study of the nanostructure of hard/soft magnetic multilayers

Matteo Amato
Dipartimento di Fisica, Università di Firenze, Largo Enrico Fermi 2, I-50125 Firenze, Italy

Maria Gloria Pini
Istituto di Elettronica Quantistica, Consiglio Nazionale delle Ricerche, Via Panciatichi 56/30, I-50127 Firenze, Italy

Angelo Rettori
Dipartimento di Fisica, Università di Firenze and Istituto Nazionale di Fisica della Materia, Unità di Firenze, Largo Enrico Fermi 2, I-50125 Firenze, Italy

(Received 16 November 1998)

We present numerical simulations, based on a mean-field calculation of the equilibrium configuration, for the magnetization reversal process in magnetic multilayers consisting of a hard (h) phase with large anisotropy, exchange coupled to a soft (s) phase with large magnetization. Starting from a trilayer made of $50h/100s/50h$ layers, and using realistic Hamiltonian parameters pertinent to epitaxial Sm-Co/Fe films, we separately investigate the effect of (i) increasing nanostructuration, while maintaining constant the overall hard/soft ratio, and (ii) decreasing the thickness of the hard phase, while keeping constant that of the soft phase. We find that the exchange-bias field and the coercive field strongly increase upon increasing nanostructuration and that the maximum energy product $(BH)_{\max}$ rapidly tends to the ideal value $(2\pi M_{\mathrm{sat}})^2$. In contrast, upon reducing the thickness of the hard phase in a trilayer, the exchange-bias field and the coercive field remain nearly constant. Thus, combining both effects in an opportune way, we are able to determine the most convenient composition in order to obtain a permanent exchange-spring magnet with high performance, i.e., very high $(BH)_{\max}$. [S0163-1829(99)02729-0]

I. INTRODUCTION

In recent years, the search for high performance permanent magnetic materials[1,2] has received strong impetus since the concept of the exchange-spring magnet was introduced.[3] The idea is to assemble a composite magnet consisting of two suitably dispersed and mutually exchange-coupled phases: a hard (h) phase, which provides a high coercive field, and a soft (s) phase, with a high saturation magnetization. The exchange coupling between the two phases gives origin to a typical reversible behavior of the demagnetization curve, hence the name exchange-spring magnet. In this way, one can obtain an enhancement of remanence with respect to a magnet made of the pure hard phase, so that high-energy products $(BH)_{\max}$ can be reached:[4] for example, in $Sm_2Fe_{17}N_3/Fe_{65}Co_{35}$ multilayers with a volume fraction of only 9% of the hard phase, Skomski and Coey predicted a $(BH)_{\max}$ as high as 137 MGOe (i.e., more than twice the value obtained by a laboratory-scale $Nd_2Fe_{14}B$ magnet[5]). The fine distribution of the two phases on a nanometric scale can be achieved by several techniques: melt spinning,[6,7] mechanical alloying,[8,9] etc. Multilayer exchange-spring magnets, which can be obtained by ultrahigh vacuum vapor deposition[10] or sputtering,[11–18] are particularly appealing from the theoretical point of view because the thicknesses of the hard and soft phases are easily controllable, thus leading to a simple and well-defined structure. Moreover, they are becoming more and more interesting even for applications, owing to the possibility of being integrated in electronic devices.[19]

In this paper, we present a theoretical study of the magnetization reversal process in a two-phase multilayer. Our work was stimulated by recent experimental results and numerical simulations in high-quality epitaxial hard/soft Sm-Co/transition metal (TM) (TM=Fe, Co) bilayers,[16,17] grown via dc magnetron sputtering.[15] To calculate the equilibrium configuration for a multilayer, we use a mean-field method recently developed.[20,21] Starting from a trilayer made of $50h/100s/50h$ layers, we separately investigate the effect of the following.

(i) Increasing nanostructuration, while maintaining constant the total number of layers and the overall hard/soft ratio, in order to obtain higher exchange-bias and coercive fields.

(ii) Decreasing the thickness of the hard phase, while keeping constant that of the soft phase, so that a higher saturation magnetization can be obtained.

Our aim is to determine the optimal composition in order to obtain a permanent exchange-spring magnet with high performance. In particular, for a Sm-Co/Fe film with opportune nanostructuration and reduction of the hard phase (actually, a $10h+33s+10h+34s+10h+33s+10h$ heptalayer), we predict that a very high maximum energy product, $(BH)_{\max} \approx 74$ MGOe, can be obtained. The paper is organized as follows. In Sec. II we present the model and the mean-field theoretical framework. In Sec. III the results of our calculation are displayed and discussed. Finally, in Sec. IV we draw the conclusions.

 ©1999 The American Physical Society

II. PRINCIPLES OF THE NUMERICAL SIMULATION

Several methods[10,14,17,22–26] can be used in the modeling of exchange-spring permanent magnets. In magnetic hard/soft multilayers with a total number of planes N, the magnetization reversal process can be simulated using a one-dimensional model: the magnetic properties are considered to be invariant inside a plane parallel to the interfaces and to depend only on the plane index i. The total energy of the system is written as

$$E=-\sum_{i=1}^{N-1}\frac{A_{i,i+1}}{d^2}\cos(\theta_i-\theta_{i+1})-\sum_{i=1}^{N}K_i\cos^2\theta_i - \sum_{i=1}^{N}HM_i\cos(\theta_i-\theta_H), \tag{1}$$

where $A_{i,i+1}$ is the exchange interaction between the ith and the $(i+1)$th planes; K_i and M_i are, respectively, the uniaxial in-plane anisotropy and the magnetic moment relative to the ith plane; d is the interplane distance and θ_i is the angle formed by the magnetization of the ith plane with the in-plane easy axis of the hard layer; a magnetic field H is applied at an angle θ_H with the in-plane easy axis. Following the paper by Jiang *et al.*,[16] we choose the Hamiltonian parameters pertinent to epitaxial Sm-Co/Fe films: $A_h=1.2\times10^{-6}$ ergs/cm, $K_h=5\times10^7$ ergs/cm^3, $M_h=550$ emu/cm^3 for the hard layer, and $A_s=2.8\times10^{-6}$ ergs/cm, $K_s=10^3$ ergs/cm^3, $M_s=1700$ emu/cm^3 for the soft ones; the interface exchange constant was taken $A_{hs}=1.8\times10^{-6}$ ergs/cm, i.e., intermediate between A_s and A_h. The interlayer constant d was set 2×10^{-8} cm.

To calculate the equilibrium configurations of the system we use a method recently developed by Trallori *et al.*,[20,21] where mean-field theory is reformulated as a nonlinear map with opportune boundary conditions. One starts by deriving Eq. (1) with respect to θ_i $(i=1,\ldots,N)$

$$\frac{\partial E}{\partial\theta_i}=0=+(1-\delta_{i,1})\frac{A_{i-1,i}}{d^2}\sin(\theta_i-\theta_{i-1}) - (1-\delta_{i,N})\frac{A_{i,i+1}}{d^2}\sin(\theta_{i+1}-\theta_i)+2K_i\cos\theta_i\sin\theta_i + HM_i\sin(\theta_i-\theta_H). \tag{2}$$

Introducing the notations $s_i=\sin(\theta_i-\theta_{i-1})$, Eq. (2) can be rewritten as a two-dimensional recursive map

$$\frac{A_{i,i+1}}{d^2}s_{i+1}=\frac{A_{i-1,i}}{d^2}s_i+2K_i\cos\theta_i\sin\theta_i+HM_i\sin(\theta_i-\theta_H)$$

$$\theta_{i+1}=\theta_i+\sin^{-1}(s_{i+1}) \tag{3}$$

with the boundary conditions

$$s_1=\sin(\theta_1-\theta_0)=0,\quad s_{N+1}=\sin(\theta_{N+1}-\theta_N)=0. \tag{4}$$

The latter equations represent two curves in the two-dimensional phase space (s,θ). Their physical meaning is related to the absence of exchange interaction on one side of each surface layer: see the Dirac δ functions in Eq. (2). Within the map formalism, the equilibrium configurations of a finite film with N planes are rigorously obtained as the trajectories—in the (s,θ) phase space—having two intersections with the boundary conditions line $s=0$, which are separated by exactly N steps of the recursive mapping. It is important to note that no approximations are involved in this procedure: i.e., the calculation is accurate within machine precision, whatever the structure of the multilayer.[27] Further details about the map method can be found in the review paper by Trallori *et al.*[21] Here we only observe that, for the chosen Hamiltonian parameters, the Zeeman and the anisotropy energies are much smaller than the exchange energy, so that the phase portrait is not chaotic, thus allowing a particularly easy determination of the equilibrium configuration.

III. MAGNETIZATION REVERSAL PROCESS: NUMERICAL RESULTS

We start from a trilayer made of $50h/100s/50h$ layers in zero field, with the magnetic moments of each plane aligned along the x axis $(\theta_i=0,\ \forall i)$, which we assume to be the in-plane easy axis for the anisotropy of the hard phase. Then we apply a negative magnetic field $(\theta_H=\pi)$ and look for the equilibrium configurations of the multilayer. We are interested in the metastable spin arrangements, which can be uniform or nonuniform, and in their evolution when the intensity of the reverse field is increased in modulus. The demagnetization curve is calculated using the spin configurations $\{\theta_i\}$, obtained by the previously described map formulation of mean-field theory:

$$\frac{M}{M_{\rm sat}}=\frac{\sum_{i=1}^{N}M_i\cos(\theta_i-\theta_H)}{\sum_{i=1}^{N}M_i}, \tag{5}$$

with $\theta_H=\pi$ and $M_{\rm sat}$ is the saturation magnetization. The longitudinal component of the reduced magnetization is shown in Fig. 1(a), while in Fig. 1(b) some spin configurations are reported at selected values of the magnetic field. For low reverse field,[28] the metastable spin configuration is found to be uniform $(\theta_i=0,\ \forall i)$: the magnetization reversal is prevented by the hard layers which pin the soft layers, due to the hard/soft exchange interaction. For reverse fields higher than the exchange-bias field $H_{\rm ex}=0.26$ T, the central soft layers start to follow the magnetic field and a strongly nonuniform spin configuration, with two domain walls, is realized [see Fig. 1(b)]: correspondingly, the parallel component of the magnetization drops sharply from the value 1. It should be noted that, in this field regime, the hard layers give only a small contribution to the decrease of the magnetization since, besides having a smaller saturation magnetization with respect to the soft phase, they are only slightly perturbed by the rotation of the soft layers. Upon increasing the reverse field, the domain walls, nucleated in the soft phase, are reversibly compressed and progressively invade the hard layers. The reversible rotation of the magnetization brings the system to zero remanence at the coercive field $H_c=0.59$ T. As the process continues, the energy associated with the domain walls in the hard layers becomes higher and higher until, at a critical value of the field, $H_{\rm irr}=1.34$ T, the

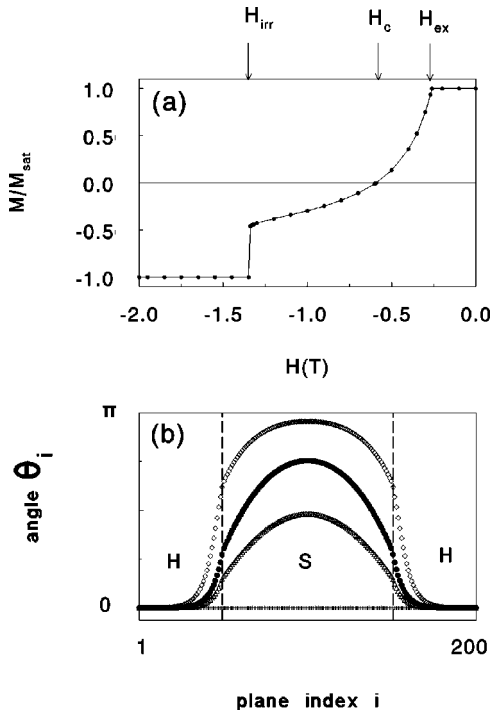

FIG. 1. (a) Circles: longitudinal component of the reduced magnetization $M/M_{\rm sat}$ of a $50h/100s/50h$ trilayer as a function of the reverse magnetic field (in Tesla). The full line is a guide to the eye. (b) Metastable spin configurations of the trilayer. Crosses (i.e., horizontal line, $\theta_i=0\ \forall i$): $H=0$. Open triangles: $H=0.35$ T ($H_c>H>H_{\rm ex}=0.26$ T). Full circles: $H=0.59$ T (H just lower than H_c). Open rhombs: $H=1.34$ T (H just lower than $H_{\rm irr}$).

spins of both the soft and hard layers switch irreversibly and the magnetization saturates to the value -1. The reason why the irreversibility field results about one order of magnitude smaller than the anisotropy field in the hard material ($H_{\rm irr}<H_h^{\rm (anis)}=2K_h/M_h=18.2$ T, with our choice of Hamiltonian parameters) was explained by Kneller and Hawig[3] in the hypothesis of high thickness of the soft phase with respect to the hard one. They pointed out that, with increasing H, the energy density of a domain wall in the soft material increases above its equilibrium value, $\epsilon_s>\epsilon_s^{\rm (eq)}\approx HM_s$, owing to the strong compression against the hard phase. The critical field $H_{\rm irr}$ is determined by the condition that the energy density in the soft material approaches that in the hard one, $\epsilon_s\to\epsilon_h\approx 2K_h$, thus leading to the reduction of the switching field with respect to the anisotropy field of the hard material: $H_{\rm irr}<2K_h/M_s<2K_h/M_h=H_h^{\rm (anis)}$.

It is interesting to compare the previous results for the $50h+100s+50h$ trilayer with those obtained in the case of a bilayer with the same total number of hard and soft layers. By the map method we find for a $100h+100s$ bilayer: $H_{\rm ex}=0.08$ T, $H_c=0.23$ T, $H_{\rm irr}=1.33$ T, in fair agreement with the experimental data in Sm-Co/Fe epitaxial bilayers.[16] It should be noted that our estimation for $H_{\rm irr}$ is not expected to be fully reliable, since the simulation is based upon the assumption of a coherent rotation of the magnetization, which is well justified only in the reversible regime. Passing from the bilayer to the trilayer, we find that the exchange-bias field $H_{\rm ex}$ and the coercive field H_c increase by a factor 3 and 2.5, respectively. Clearly, this is due to the fact that, in

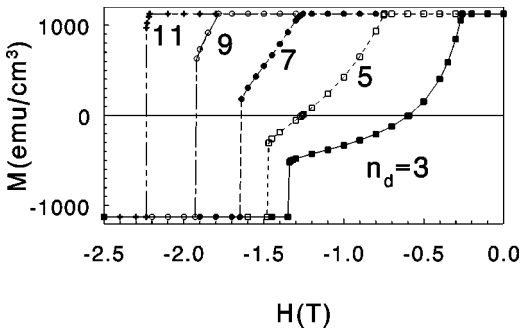

FIG. 2. Symbols: calculated demagnetization curves for various films, all with the same total number of layers, $N=N_h+N_s=200$, and the same total hard to soft ratio $r=N_h/N_s=1$, but different nanodispersion index n_d (i.e., $n_d=3$ denotes a $h/s/h$ trilayer, $n_d=5$ a $h/s/h/s/h$ pentalayer, etc.: see Sec. III A). The lines are guides to the eye.

the $50h+100s+50h$ trilayer, the reversal of the magnetization in the soft material is more hampered owing to the presence of the hard material, exchange-coupled to the soft one, on both sides. In contrast, the irreversibility field $H_{\rm irr}$ in the trilayer is only 1% greater than in the bilayer: in fact, on the basis of the mechanism discussed above, $H_{\rm irr}$ is not expected to vary in a substantial way, as long as the thickness of the soft phase is appreciably greater than that of the hard phase.

A. Effect of increasing nanostructuration

The previous findings regarding the trilayer-versus-bilayer behavior induced us to further investigate the effect of increasing nanostructuration while maintaining constant the total number of hard and soft layers: $N=N_h+N_s=200$ and the overall hard/soft ratio: $r=N_h/N_s=1$, where $N_h=\Sigma_i N_{i,h}=100$ and $N_s=\Sigma_i N_{i,s}=100$. In Fig. 2 we present the results of our numerical simulations for the magnetization reversal in the case of a pentalayer ($n_d=5$): $33h+50s+34h+50s+33h$; a heptalayer ($n_d=7$): $25h+33s+25h+34s+25h+33s+25h$; an ennealayer ($n_d=9$): $20h+25s+20h+25s+20h+25s+20h+25s+20h$; and an endecalayer ($n_d=11$): $17h+20h+17h+20s+16h+20s+16h+20s+17h+20s+17h$.

We denote by n_d the nanodispersion index, so that $n_d=5$ for the pentalayer, $n_d=7$ for the heptalayer, and so on. It is apparent that, upon increasing nanostructuration, the exchange-bias field $H_{\rm ex}$ increases and the convexity of the demagnetization curve $M(H)$ changes, approaching that of a ''normal'' permanent magnet as n_d increases.[3] Actually, the higher the nanostructuration, the smaller the thickness of the soft phase: see Fig. 3, where the equilibrium spin configurations are reported for different values of n_d (and at $H\lesssim H_c$). Thus, the anisotropy of the hard phase is more effective (through the hard-soft exchange interaction) on the spins of the soft layers. On one side, the exchange-bias field $H_{\rm ex}$ increases with increasing n_d, i.e., the uniform configuration is more favored, since the soft layers are more and more pinned by the hard ones. On the other side, when domain walls begin to form in the system, the higher is n_d the sooner they become unstable, leading to an irreversibility of the demagnetization process, with a change of convexity of the $M(H)$ curve.[3] In Fig. 4(a) we report the exchange-bias field

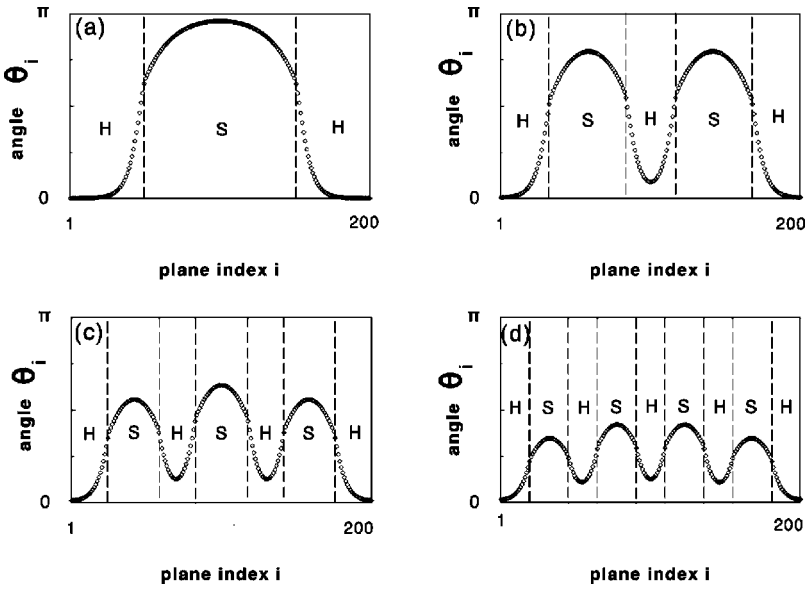

FIG. 3. Calculated metastable spin configurations of various films, all with $N=N_h+N_s=200$ and $r=N_H/N_s=1$, but different nanodispersion index n_d: (a) $n_d=3$, $H=1.34$ T; (b) $n_d=5$, $H=1.47$ T; (c) $n_d=7$, $H=1.65$ T; (d) $n_d=9$, $H=1.92$ T. In all cases, the field was chosen to be just smaller than the irreversibility field $H_{\rm irr}$.

$H_{\rm ex}$, the coercive field H_c, and the irreversibility field $H_{\rm irr}$ versus n_d. The qualitative features previously deduced from the comparison between the bilayer and the trilayer are confirmed by our detailed analysis; e.g., on passing from the trilayer to the endecalayer, we observe a strong increase, by nearly an order of magnitude, of the exchange-bias field $H_{\rm ex}$. It is worth noticing that our numerical results for $H_{\rm ex}$ turn out to be in excellent agreement[29] with the solutions for the nucleation field H_N, obtained solving the implicit equation (11) in the paper by Skomsky and Coey.[4] These authors considered a multilayered structure of alternating soft and hard magnetic layers with sufficiently small multilayer periodicity ($\leqslant 10$ nm), a condition which is fulfilled by our model. Also the coercive field H_c is found to strongly increase upon increasing nanostructuration. The irreversibility field $H_{\rm irr}$ remains nearly constant as long as the thickness of the soft phase is substantially greater than that of the hard phase (in practice for $n_d \leqslant 7$); with a further increase of n_d, $H_{\rm irr}$ increases almost linearly.

We observe that, in order to calculate the exchange-bias field $H_{\rm ex}$, it is not necessary to solve the map equations Eq. (3) with the boundary conditions Eq. (4), but it is sufficient to determine the eigenvalues of the Hessian $(\partial^2 E/\partial\theta_i\partial\theta_j)$ $(i,j=1,\ldots,N)$. As long as they are all positive [i.e., the form (1) is positive definite], the uniform configuration with all the spins aligned opposite to the field is a relative minimum of the energy (1); the field for which at least one of the eigenvalues becomes negative is $H_{\rm ex}$. In contrast, to calculate H_c and $H_{\rm irr}$, one has to actually find the trajectories in the phase space satisfying Eq. (3) and Eq. (4). We note that for $n_d \geqslant 7$, H_c coincides with $H_{\rm irr}$: i.e., already for the heptalayer the reversal of the magnetization takes place in a nonreversible way before M has reached the zero value. Moreover we find that for $n_d \geqslant 13$ (not shown in Fig. 2) the three fields coincide: $H_{\rm ex}=H_c=H_{\rm irr}$, i.e., the magnetization reversal from the $+1$ to the -1 value occurs abruptly; experimentally, one should observe a perfectly square hysteresis cycle.

Next, it is worthwhile investigating the effect of nanodispersion on the energy-product $(BH)_{\rm max}$. The latter represents the figure of merit for a permanent magnet material, since it measures its ability to produce a large magnetic field (large remanence) for an extended period of time (large coercive field). From our simulations of the demagnetization curve, we can easily calculate the energy product $BH=(4\pi M-H)H$ (where the field H is considered as positive) and find for which value of H it is maximum. In Fig. 4(b), we report the calculated $(BH)_{\rm max}$ versus the nanodispersion index n_d, together with the ideal value $(BH)_{\rm max}^{\rm ideal}$

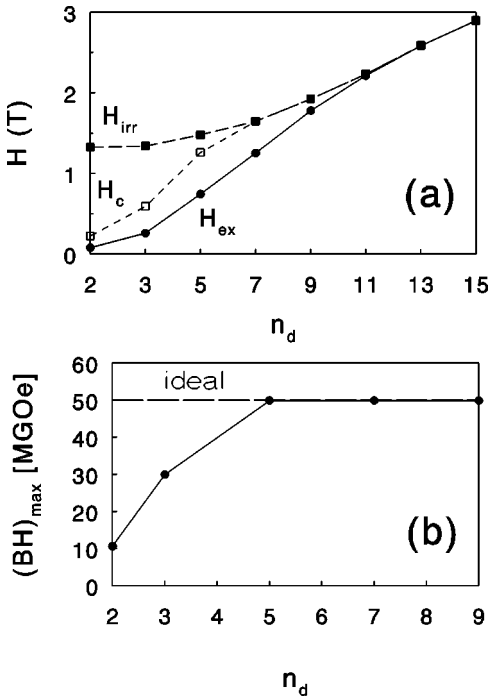

FIG. 4. (a) $H_{\rm ex}$ (exchange-bias field, at which the magnetization drops sharply from the value 1), H_c (coercive field, at which $M=0$) and $H_{\rm irr}$ (irreversibility field, at which the magnetization undergoes a sudden reversal to negative saturation) reported as a function of the nanodispersion index n_d. (b) Calculated maximum energy product $(BH)_{\rm max}$ (full circles) as a function of the nanodispersion index n_d, compared with the constant, ideal one (dashed line): $(BH)_{\rm max}^{\rm ideal}=(2\pi M_{\rm sat})^2$. The full line is a guide to the eye.

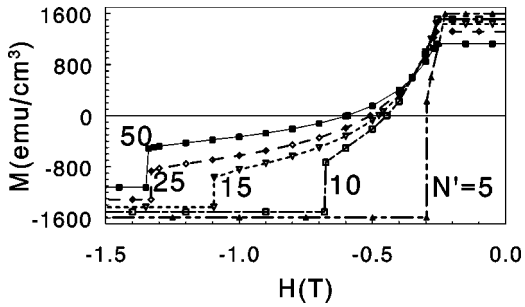

FIG. 5. Symbols: calculated demagnetization curves of trilayers ($n_d=3$) of the type $N'h/100s/N'h$, for selected values of N', ranging between 50 and 5. The lines are guides to the eye.

$=(2\pi M_{\rm sat})^2$, pertinent to a square hysteresis loop (i.e., a linear B versus H plot), and corresponding to $H^{(\rm ideal)}=B^{(\rm ideal)}=2\pi M_{\rm sat}$. We observe that for a film made of N_h hard layers and N_s soft layers, with magnetizations M_h and M_s, respectively, the saturation magnetization is given by

$$M_{\rm sat}=\frac{N_hM_h+N_sM_s}{N_h+N_s}. \tag{6}$$

For a film with $N_h=N_s=100$ and magnetizations $M_h=550$ emu/cm^3, $M_s=1700$ emu/cm^3, we obtain $M_{\rm sat}=1125$ emu/cm^3, so that $H^{(\rm ideal)}=2\pi M_{\rm sat}=7.068$ kOe. As a consequence we have that, if the demagnetization curve keeps on to be saturated up to an exchange-bias field $H_{\rm ex}$ higher than $H^{(\rm ideal)}=2\pi M_{\rm sat}$, the calculated maximum energy product $(BH)_{\rm max}$ turns out to be equal to the ideal value, which for $N_h=N_s=100$ is nearly 50 MGOe. In practice, this happens already for the pentalayer, since it has $H_{\rm ex}=7.466$ kOe. We note that the previous estimation for $H_{\rm ex}$ is expected to be reliable since in the case $n_d=5$ one has $H_{\rm ex}\ll H_{\rm irr}$. Thus we conclude that, from the point of view of the maximum energy product, in the case of an overall hard/soft ratio $r=N_h/N_s=1$ it seems not convenient to pursue nanostructuration beyond $n_d=5$.

B. Effect of decreasing the thickness of the hard phase

One of the technological advantages of exchange-spring magnets is that they contain less rare-earth (RE) content than single-component hard RE-TM intermetallics, with the effect of lowering the cost of materials and improving resistance to corrosion. Thus, it is quite important to investigate the effect of lowering the thickness of the expensive RE component in an exchange-spring magnet.

In Fig. 5 we present the results of our numerical simulations for the magnetization reversal in the case of a symmetric trilayer ($n_d=3$) of the type $N'h/100s/N'h$, i.e., with a fixed number (100) of soft layers and with a number N' of hard layers on each side of the soft slab, which we allow to vary between 50 and 5. In Fig. 6 the evolution of the equilibrium spin configuration is shown as a function of N' for a field value, $H=0.6$ T, which is greater than the coercive field H_c for all the considered values of N'. It is well known[22,10,14] that, for low values of N', the boundary conditions $\theta_1=\theta_N=0$ or π, corresponding to infinite anisotropy in the hard layer (or infinite thickness of the hard layer, $N'\to\infty$) and ideal exchange coupling at the interfaces, can be inadequate. An advantage of our method is that it does not make any approximation about the magnetization direction of the two surface planes. In fact, for sufficiently high fields ($H_c\lesssim H$), we find that the deviation from 0 of the magnetization of the outermost plane increases in a significant way upon decreasing N': see Fig. 6.

In Fig. 7(a), the three fields $H_{\rm ex}$, H_c, and $H_{\rm irr}$ are reported as a function of N'. The decrease in $H_{\rm ex}$ is very smooth for decreasing N' because the value of $H_{\rm ex}$ is essentially determined by the pinning effect of the anisotropy of the hard phase on the magnetization of the soft phase, which is nearly the same for the investigated series of trilayers. Also the coercive field H_c is found to increase very smoothly with increasing N': thus, one can infer that there is not much use in increasing the thickness of the hard phase in the effort to improve the performance of the exchange-spring magnet. Finally, the decrease in $H_{\rm irr}$ with decreasing N' is expected. In fact, the lower is N' the higher is the cost (per spin) in exchange and anisotropy energy for a domain wall in the

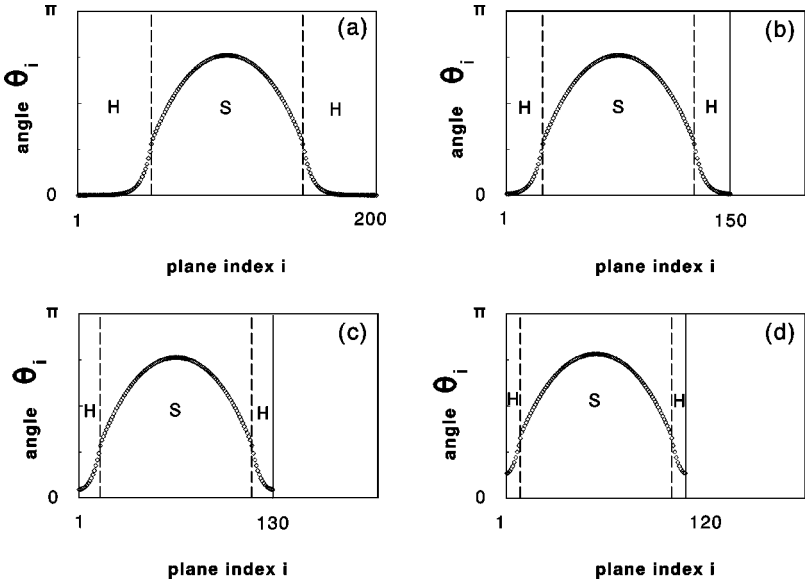

FIG. 6. Calculated metastable spin configurations of trilayers ($n_d=3$) of the type $N'h/100s/N'h$ for selected values of N'. (a) $N'=50$; (b) $N'=25$; (c) $N'=15$; (d) $N'=10$. The reverse magnetic field was fixed to the value $H=0.6$ T (i.e., $H_c<H<H_{\rm irr}$, for all the considered values of N').

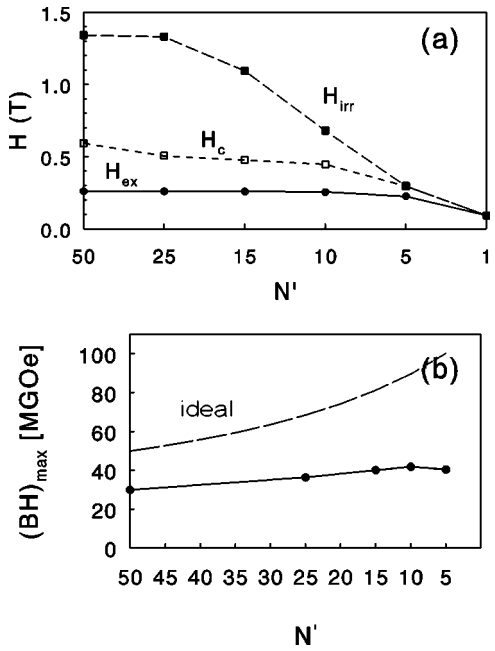

FIG. 7. (a) H_{ex}, H_c, and H_{irr} reported as a function of N' for trilayers of the type $N'h/100s/N'h$. (b) Calculated maximum energy product $(BH)_{max}$ (full circles), for trilayers of the type $N'h/100s/N'h$ as a function of N', compared with the ideal one (dashed line). The full line is a guide to the eye.

hard phase (see Fig. 6), so that the irreversible switch of the magnetization takes place for lower field.

Let us now investigate how the figure of merit of the permanent magnet depends on N'. In Fig. 7(b) we report the calculated energy product $(BH)_{max}$ as a function of N', in comparison with the ideal value $(BH)_{max}^{ideal}=(2\pi M_{sat})^2$. We observe that the saturation magnetization, given by Eq. (6) with $N_h=2N'$, can be rewritten as

$$M_{sat}=M_h+\frac{N_s(M_s-M_h)}{2N'+N_s}. \tag{7}$$

Thus, M_{sat} monotonically increases with decreasing N', and so does the ideal energy product. In contrast, the calculated $(BH)_{max}$ presents a very smooth dependence on N' (with a rounded maximum at $N'=10$), as expected on the basis of the nearly constant dependence of H_{ex} on N' [see Figs. 5 and 7(a)].

Finally, it is worth noting that recently micromagnetic calculations of the nucleation field H_N and of the maximum energy product in h/s/h trilayers were performed by Leineweber and Kronmüller.[26] However, since these quantities were expressed as a function of the soft layer thickness d_s, a direct comparison with our results is prevented, even though their correct order of magnitude is recovered in the appropriate regime $2d_s \gg \pi\delta_h$, where, in our notations, $\delta_h=\sqrt{A_h/2K_h}$ is the domain-wall thickness in the hard phase (for our model, $2d_s=40$ nm, while $\delta_h \approx 1$ nm).

IV. CONCLUSIONS

In the previous sections we showed that, upon varying the thickness and the arrangement of the hard and soft phases, it is possible to modulate the properties of a multilayer exchange-spring magnet, i.e., the values of the exchange-bias field H_{ex}, the coercive field H_c and the irreversibility field H_{irr}, in an almost continuous way. In particular we found that, upon increasing nanostructuration, the maximum energy product $(BH)_{max}$ rapidly tends to the ideal value $(2\pi M_{sat})^2$. On the other hand, upon reducing the thickness of the hard phase in an $N'h/100s/N'$ trilayer, we found that $(BH)_{max}$ presents a rather smooth behavior. These findings suggest that, upon variation of both the nanodispersion index n_d and the thickness of the hard phase, it should be possible to determine the optimal composition of the exchange-spring multilayer magnet, in order to meet the requirements for applications. In practice, whenever the condition $H_{ex} > 2\pi M_{sat}$ is fulfilled, the maximum energy product turns out to be equal to the ideal value. It is extremely easy to calculate H_{ex}: it suffices diagonalizing the $N\times N$ matrix of the Hessian $(\partial^2 E/\partial\theta_i\partial\theta_j)$ $(i,j=1,\ldots,N)$. The smallest value of the applied field for which at least one, out of the N eigenvalues, becomes negative is just H_{ex}. For example, in the case of a heptalayer $(n_d=7)$, we find that upon reduction of the global thickness of the hard phase from $N_h=100$ to $N_h=40$ (i.e., realizing the $10h+33s+10h+34s+10h+33s+10h$ arrangement), the field of magnetization reversal H_{ex} decreases from 12.5 kOe [see Fig. 4(a)] to 10.7 kOe, while the quantity $2\pi M_{sat}$ increases from 7.068 kG to 8.617 kG. Then, for the above-mentioned heptalayer with reduced hard-phase content with respect to that considered in Sec. III A, the maximum energy product $(BH)_{max}$ turns out to be 74 MGOe, i.e., a value sensibly higher than that obtained by a laboratory-scale $Nd_2Fe_{14}B$ magnet.[5]

It is interesting to note that a maximum energy product of the same order (73 MGOe) was predicted by Fullerton *et al.*[17] (see Fig. 11 of their paper) in the case of a Sm-Co/Fe bilayer with rather small layer thicknesses: 12 Å for the hard phase and 40 Å for the soft one. For a model of spherical Fe inclusions in Sm-Co, an even higher maximum energy product ($\approx$86 MGOe) can be estimated in the framework of the theory by Skomsky and Coey[4] [see Eq. (9) in their paper], provided that the diameter of the soft inclusion is smaller than a few nm. We observe that a further increase of the energy product is possible if the soft Fe phase is replaced by Co, which has higher saturation magnetization M_s, exchange constant A_s, and uniaxial anisotropy K_s.

In conclusion, from our numerical analysis, we found that multilayer exchange-spring magnets with a considerable maximum-energy product $(BH)_{max}$ can be obtained using a rather small quantity of hard material, provided that nanostructuration is high enough. Clearly, to determine the form of the demagnetization curve $M(H)$, a more detailed analysis is required; we showed that, at low temperatures, our reformulation of mean-field theory as a nonlinear map with opportune boundary conditions[20,21] allows a very rapid and precise determination of the equilibrium configuration of the multilayer, and thus an accurate simulation of the $M(H)$ curve.

ACKNOWLEDGMENTS

We thank G. Asti and M. Solzi for fruitful discussions.

[1] G. Asti and M. Solzi, in *Applied Magnetism*, edited by R. Gerber, C. D. Wright, and G. Asti (Kluwer, Dordrecht, 1994), pp. 309–376.
[2] M. Solzi, in *Magnetic Properties of Matter*, edited by L. Lanotte, F. Lucari, and L. Pareti (World Scientific, Singapore, 1996), pp. 191–199.
[3] E. F. Kneller and R. Hawig, IEEE Trans. Magn. **27**, 3588 (1991).
[4] R. Skomski and J. M. D. Coey, Phys. Rev. B **48**, 15 812 (1993); see also, R. Skomsky and J. M. D. Coey, IEEE Trans. Magn. **29**, 2860 (1993); J. M. D. Coey and R. Skomsky, Phys. Scr. **T49**, 315 (1993); J. M. D. Coey, J. Magn. Magn. Mater. **140-144**, 1041 (1995); Solid State Commun. **102**, 101 (1997).
[5] M. Sagawa, S. Hirosawa, H. Yamamoto, S. Fujimura, and Y. Matsuura, Jpn. J. Appl. Phys., Part 1 **26**, 785 (1987).
[6] L. Withanawasam, A. S. Murphy, G. C. Hadjipanayis, and R. F. Krause, J. Appl. Phys. **76**, 7065 (1994).
[7] C. J. Yang and E. B. Park, IEEE Trans. Magn. **32**, 4428 (1996).
[8] J. Ding, P. G. McCormick, and R. Street, J. Magn. Magn. Mater. **124**, 1 (1993); J. Ding, Y. Liu, R. Street, and P. G. McCormick, J. Appl. Phys. **75**, 1032 (1994); P. G. McCormick, W. F. Miao, P. A. I. Smith, J. Ding, and R. Street, *ibid.* **83**, 6256 (1998).
[9] K. O'Donnel, C. Khurt, and J. M. D. Coey, J. Appl. Phys. **76**, 7068 (1994).
[10] K. Mibu, T. Nagahama, and T. Shinjo, J. Magn. Magn. Mater. **163**, 75 (1996).
[11] I. A. Al-Omari and D. J. Sellmyer, Phys. Rev. B **52**, 3441 (1995).
[12] S. M. Parhofer, J. Wecker, C. Kuhrt, G. Gieres, and L. Schultz, IEEE Trans. Magn. **32**, 4437 (1996).
[13] M. Shindo, M. Ishizone, A. Sakuma, H. Kato, and T. Miyazaki, J. Appl. Phys. **81**, 4444 (1997).
[14] S. Wüchner, J. C. Toussaint, and J. Voiron, Phys. Rev. B **55**, 11 576 (1997).
[15] E. E. Fullerton, C. H. Sowers, J. P. Pearson, S. D. Bader, X. Z. Wu, and D. Lederman, Appl. Phys. Lett. **69**, 2438 (1996); E. E. Fullerton, C. H. Sowers, X. Z. Wu, and S. D. Bader, IEEE Trans. Magn. **32**, 4434 (1996); E. E. Fullerton, J. S. Jiang, C. Rehm, C. H. Sowers, S. D. Bader, J. B. Patel, and X. Z. Zu, Appl. Phys. Lett. **71**, 1579 (1997).
[16] J. S. Jiang, E. E. Fullerton, M. Grimsditch, C. H. Sowers, and S. D. Bader, J. Appl. Phys. **83**, 6238 (1998).
[17] E. E. Fullerton, J. S. Jiang, M. Grimsditch, C. H. Sowers, and S. D. Bader, Phys. Rev. B **58**, 12 193 (1998).
[18] E. E. Fullerton, J. S. Jiang, C. H. Sowers, J. E. Pearson, and S. D. Bader, Appl. Phys. Lett. **72**, 380 (1998).
[19] G. A. Prinz, Phys. Today **48** (4), 58 (1995).
[20] L. Trallori, P. Politi, A. Rettori, M. G. Pini, and J. Villain, Phys. Rev. Lett. **72**, 1925 (1994).
[21] L. Trallori, M. G. Pini, A. Rettori, M. Macciò, and P. Politi, Int. J. Mod. Phys. B **10**, 1935 (1996).
[22] E. Goto, N. Nayashi, T. Miyashita, and K. Nakagawa, J. Appl. Phys. **36**, 2951 (1965).
[23] R. E. Camley, Phys. Rev. B **35**, 3608 (1987); R. E. Camley and D. R. Tilley, *ibid.* **37**, 3413 (1988); R. E. Camley, *ibid.* **39**, 12 316 (1989).
[24] M. Motokawa and H. Dohnomae, J. Phys. Soc. Jpn. **60**, 1355 (1991).
[25] T. Schrefl, J. Fidler, and H. Kronmüller, Phys. Rev. B **49**, 6100 (1994); T. Schrefl and J. Fidler, J. Magn. Magn. Mater. **177-181**, 970 (1998); T. Schrefl and J. Fidler, J. Appl. Phys. **83**, 6262 (1998).
[26] T. Leineweber and H. Kronmüller, Phys. Status Solidi B **201**, 291 (1997); J. Magn. Magn. Mater. **176**, 145 (1997).
[27] Moreover, by our method, the equilibrium configuration can be determined without having to postulate a misalignment between the field and the easy axis.
[28] Hereafter, and in the figure captions, we always refer to the absolute values of the fields.
[29] For example, for the pentalayer we find $H_{ex}=0.7465$ T, while the calculated H_N is 0.7434 T; for the endecalayer we have $H_{ex}=2.2137$ T, to be compared with $H_N=2.2064$ T.